

## ENERGY AND PARTICLE TRANSPORT IN MEDIUM-DENSITY ASDEX PELLET DISCHARGES

O. Gruber, W. Jilge, V. Mertens, G. Vlases, M. Kaufmann, R. Lang, W. Sandmann, K. Büchl, H.S. Bosch, H. Brocken, A. Eberhagen, G. Fussmann, O. Gehre, J. Gernhardt, G. v. Gierke, E. Glock, G. Haas, J. Hofmann, G. Janeschitz, F. Karger, M. Keilhacker, O. Klüber, M. Kornherr, K. Lackner, M. Lenoci, G. Lisitano, F. Mast, H. M. Mayer, K. McCormick, D. Meisel, E. R. Müller, H. Murmann, H. Niedermeyer, W. Poschenrieder, H. Rapp, H. Röhr, F. Ryter, F. Schneider, C. Setzensack, G. Siller, P. Smeulders, F. X. Söldner, K.-H. Stever, F. Wagner, D. Zasche.

Max-Planck-Institut für Plasmaphysik, EURATOM Association,  
D-8046 Garching, Fed. Rep. Germany.

### 1. INTRODUCTION

In ASDEX a comparison of ohmically heated divertor discharges with gas fuelling (GF) and pellet fuelling (PF), without any gas puffing after a gas puff "start-up" phase, has been done [1].

With a large interval between successive pellets ( $\Delta t_p \approx 40$  ms) the density stayed below  $2 \cdot 10^{19} \text{ m}^{-3}$  and only small differences resulted in the radial plasma parameter profiles and the transport behaviour comparing PF and GF discharges at the same density. With  $\Delta t_p \approx 35$  ms a medium density of  $\bar{n}_e \approx 3.3 \cdot 10^{19} \text{ m}^{-3}$  resulted where the pellet penetration depth increased up to  $\geq 25$  cm, primarily a consequence of the continuously falling electron temperature (shot PM). The PM density profiles are much more peaked than the profiles of the gas-fuelled discharge GC at the same density  $\bar{n}_e$ , whereas the PM  $T_e$  profiles become only slightly broader compared with the GC  $T_e$  profiles (see Fig. 1). The corresponding  $T_e(o)/\langle T_e \rangle$  values for both discharges are still within the scatter of the data showing profile consistency at the corresponding  $q_a^* = 3.4 : T_{e0}/\langle T_e \rangle = 2.2 \div 2.7$  [2]. In the PM discharge a distinct increase of the totally radiated power and of the radiation power density in the plasma centre is observed and sawteeth are absent after 1.1 s. With still further reduced  $\Delta t_p < 33$  ms the density is limited to  $< 5 \cdot 10^{19} \text{ m}^{-3}$  by a radiation collapse and is comparable with the density limit of a GF discharge. Only combining pellet injection and gas puffing and using wall carbonization considerably higher densities can be obtained [3].

This paper deals with a detailed comparison of the radial transport of the PM and the GC discharges with the transport analysis code TRANSP [4] using the measured radial profiles of  $n_e$ ,  $T_e$  and radiation losses.

## 2. PARTICLE TRANSPORT

In the PF discharges the particle fluxes  $\Gamma$  inside  $r < 0.75a$  are solely determined by the decrease of the particle content after the pellet injection event, which is equal to the pellet fuelling rate there. Only for larger  $r > 3/4a$  has the particle recycling flux (and the gas puff rate in GF discharges) to be considered as an additional source term. From the calculated  $\Gamma$  at  $r = 30$  cm (Fig. 2) a  $\dot{N} = \Gamma \cdot 2\pi R \cdot 2\pi r = 10^{21} \text{ s}^{-1}$  is obtained therefore, which is equal to  $\Delta N_{\text{pellet}}/\Delta t_p$ . The total particle confinement time has been estimated from pressure measurements in the divertor chamber to increase from 60 ms (GC) to about 100 ms (PM), yielding only a small recycling flux  $2 \cdot 10^{19} \text{ m}^{-2} \text{ s}^{-1}$  at  $r = a$  in the latter case.

The particle flux  $\Gamma$  can be modelled by the ansatz  $\Gamma(r, t) = -D \frac{\partial n}{\partial r} - n v_{in}$ , where  $v_{in}$  is an anomalous "inward drift" velocity. Fits have been tried to yield a consistent description of  $D$  and  $v_{in}$  over a pellet cycle by using 1)  $v_{in} = v(a)r^2/a^2$ , yielding  $D(r, t)$ , 2)  $v_{in} = 3 \frac{r^2}{a^2} D$ , yielding  $D$ , 3)  $D = 4000 \text{ cm}^2/\text{s}$ , yielding  $v(r, t)$  and 4)  $D = 0.2 \div 0.4 \chi_e$ , yielding again  $v$ . The electron thermal diffusivity  $\chi_e$  was determined from the energy transport analysis (s. Sec. 3). In practice scatter is large, but model 3) can be excluded and models 2) and 4) give about equal results for  $D$  and  $v$ , correspondingly. The same model,  $D = 0.3 \chi_e$  and  $v_{in} = 3 \frac{r^2}{a^2} D$ , describes also GF discharges with constant or rising density [5].

## 3. ENERGY TRANSPORT

The global energy confinement time  $\tau_E^* = W_{pl}/(P_{\text{heat}} - \dot{W}_{pl})$  are degraded in the PM discharge from 72 ms (GC) to a pellet-cycle-averaged value of 44 ms due to three effects:

1. The total plasma energy is smaller in PM as the temperatures are decreased and the density profiles are strongly peaked (accounting for 20% of the decrease in  $\tau_E^*$ ).
2. Radiation losses are increased from 110 kW (GC) to 160 kW (PM) (accounting for 10%) (see Fig. 3).
3. Non-adiabatic fast losses ( $\Delta W \leq 2$  kJ) occur after each pellet event constituting a time-averaged loss rate of about 50 kW for the quasi-steady PF discharge state (accounting for 10%). This energy loss is an order of magnitude higher than the energy required to ionize all injected particles. It is further equal to the time-averaged energy increase during the pellet cycle shown in Fig. 3a for the quasi-steady discharge phase.

Due to the deep pellet fuelling the convective energy losses  $P_{\text{conv}} = \frac{5}{2} k(T_e + T_i) \Gamma$  exceed the electron conduction losses throughout the plasma in contrast to the GF discharges ( $P_{\text{cond},e} \gg P_{\text{conv}}, P_{\text{rad}}$  for  $\bar{n}_e < 3 \cdot 10^{19} \text{ m}^{-3}$ ; Fig. 3b). The cycle-averaged  $\beta$  and  $\beta_p + k/2$  values of the kinetic analysis agree with the magnetic measurements.

The local transport analysis shows further that within the error bars the cycle-averaged thermal heat diffusivity  $\bar{\chi}_e^t$  can be described by the scaling  $\chi_{CMG} \sim (n_e^{0.8} T_e \eta)^{-1}$  derived from GF discharges [5], showing no major change in the anomalous transport mechanism. But  $\chi_e$  is larger than  $\chi_{CMG}$  just after the pellet injection event ( $t = t_p$ ) and smaller at the end of

the pellet cycle ( $t = t_p + \Delta t_p$ ) (Fig. 4). On the other hand, the ohmic input power is strongly changing over one pellet cycle, too, due to the  $T_e$  decrease at the pellet injection event and the corresponding increase of the loop voltage  $U_L$  (e.g.  $t_p + 5$  ms:  $P(\text{OHM}) = 650$  kW,  $t_p + \Delta t_p$ :  $P(\text{OHM}) = 450$  kW). Therefore a description  $\chi_e \sim (P_{\text{cond},e}/2\pi R)/(n_e T_e \frac{r}{T_e} \frac{\partial T_e}{\partial r})$ , where  $P_{\text{cond},e}$  is a certain fraction of the input power  $P(\text{OHM}) = U_L \cdot I$  and  $\frac{r}{T_e} \frac{\partial T_e}{\partial r} \sim \frac{r^2}{r^2}$  is fixed by the profile consistency (s. Fig. 1;  $r^*$  may be the  $q = 2$  radius), is strongly suggested and supported by the results given in Fig. 4b. One then obtains a local diffusivity  $\chi_e \sim B_t U_L r^{*2}/(R^2 n_e T_e q)$  which is derived under the assumption of profile consistency and is essentially equal to  $\chi_{\text{CMG}} = 3.4 \cdot 10^{15} B_t a / (R n_e^{0.8} T_e q)$  [ $\text{m}^2/\text{s}$ ,  $T$ , m, keV] with  $U_L \sim a \cdot R/r^{*2}$ . The ion heat conductivity is about one to two times the neoclassical one and much smaller than  $\chi_e$  both for PM and GC discharges.

## REFERENCES

- [1] G. Vlases et al, Proc. 12th Europ. Conf. on Contr. Fusion and Plasma Physics, Budapest 1985, 1 (1985) 78.
- [2] F. Wagner, O. Gruber et al, submitted to Phys.Rev.Letters.
- [3] H. Niedermeyer et al. and M. Kaufmann et al, (Invited paper), this conference.
- [4] R. Hawryluk, in *Physics of Plasmas Close to Thermonuclear Conditions*, Vol. 1, Varenna (1979) (EUR-FU-BRU/XII/476/80).
- [5] O. Gruber, Proc. Invited Papers, Int. Conf. on Plasma Physics, Lausanne (1984) Vol. 1, p. 67.

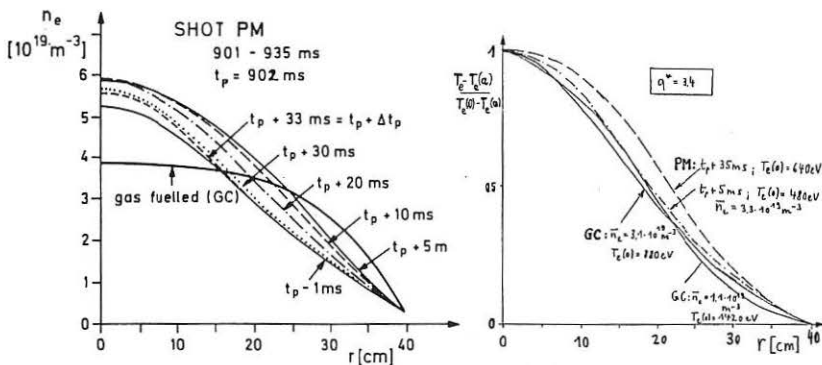


Fig. 1 Radial density and normalized temperature profiles for pellet-fuelled (PM) and a gas-fuelled (GC) discharge.

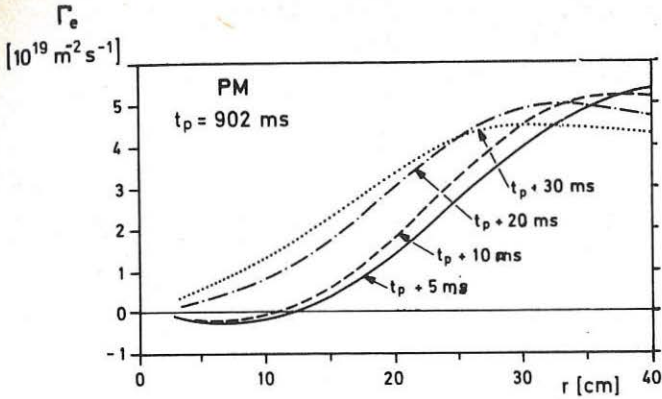


Fig. 2 Particle fluxes  $\Gamma(r, t)$  for PM discharge.

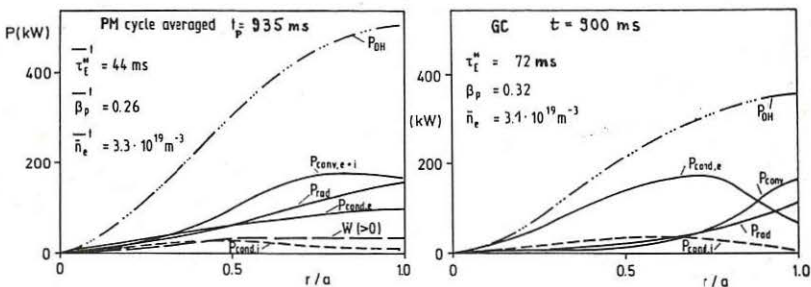


Fig. 3 Radial power balance for PM (time-averaged over a pellet cycle) and GC

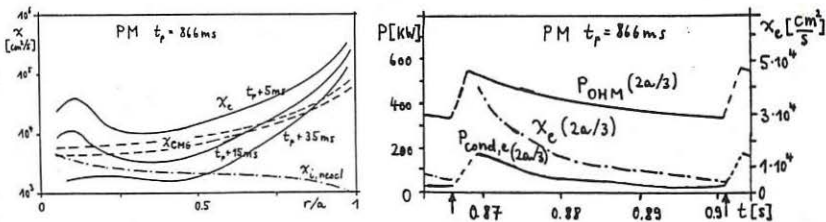


Fig. 4a Radial profiles of electron thermal diffusivity  $\chi_e$ ,  $\chi_{CMG}$  [5] for the measured plasma parameters and the neoclassical ion heat conductivity  $\chi_{i,neocl}$  (PM)  
 Fig. 4b Time dependence of ohmic heating power  $P_{OHM}$  within  $r = 2a/3$ , electron thermal conduction loss  $P_{cond,e}$  and  $\chi_e$  at  $r = 2a/3$  (PM discharge).